中國機械工程學刊第三十九卷第一期第 1~9 頁(民國一百零七年)
Journal of the Chinese Society of Mechanical Engineers, Vol.39, No.1, pp 1~9 (2018)

Effects of Annealing on Nanoindentation Behaviour and Compounds Formation of Ti/GaAs Thin Film

Woei-Shyan Lee* and Chung-Chia Lo **

Keywords: Nanoindentation, GaAs, Microstructural evolution, Annealing, Thin films.

ABSTRACT

The mechanical properties of as-deposited Ti/GaAs thin films and Ti/GaAs thin films annealed at a temperature of 490ºC for 36 minutes are investigated by means of nanoindentation tests performed to a depth of 200 nm under room temperature (RT) conditions. The microstructures of the as-deposited and annealed Ti/GaAs films are examined using scanning electron microscopy (SEM), transmission electron microscopy (TEM) and Raman scattering spectroscopy. In the nanoindentation tests, a pop-in event is observed in the loading-depth curve of the as-deposited specimen. By contrast, the loading-depth curve of the annealed specimen is continuous and smooth. The TEM results suggest that the pop-in event in the as-deposited specimen is the result of the formation of dislocations in the indented microstructure, which leads to a plastic deformation mode. Dislocation structures are also observed in the annealed specimen even though no pop-in event occurs in the loading-depth curve (i.e., the sample undergoes elastic deformation). In this case, the dislocations are thought to be related to the density of the native defects in the GaAs substrate and the difference in doping. The nanoindentation test results show that the as-deposited film has a hardness and Young's modulus of 8.90 GPa and 124.01 GPa, respectively. For the annealed specimen, the hardness and Young's modulus values increase slightly to 10.44 GPa and 124.3 GPa, respectively. The TEM observation results show that Ti_2Ga_3 and TiAs layers are formed at the interface between the Ti thin film and the GaAs substrate during the annealing process. The Raman spectroscopy analysis results show that the Raman spectrum for the as-deposited specimen has a prominent peak associated with the GaAs substrate at 268 cm^{-1}. By contrast, the Raman spectrum for the annealed sample shows a prominent peak associated with the Ti_2Ga_3 layer at 455 cm^{-1}.

Paper Received December 2017. Revised January, 2018, Accepted February, 2018, Author for Correspondence: Woei-Shyan Lee.

* *Distinguished Professor, Department of Mechanical Engineering, National Cheng Kung University, Tainan, Taiwan 70101, ROC.*

** *Graduate Student, Department of Mechanical Engineering, National Cheng Kung University, Tainan, Taiwan 70101, ROC.*

INTRODUCTION

Gallium arsenide (GaAs), a Ⅲ - Ⅴ direct bandgap semiconductor with a zinc blende crystal structure, is widely used in the fabrication of displays, sensors, light-emitting diodes (LEDs), and solar cells (Yugang *et al.*, 2005; Nakamura, 2002). In the past, GaAs was generally patterned with platinum (Pt) electrodes due to the stable Schottky contact effect. However, at high temperatures (e.g., 500ºC), the Pt/GaAs structure is damaged by Pt diffusion into the GaAs substrate, and hence diode failure occurs (Sehgal *et al.*, 1997; Donzelli, 1987; Sinha *et al.*, 1976). Accordingly, GaAs has more recently been patterned with titanium (Ti) electrodes since research has shown that the formation of interfacial TiAs under annealing temperatures prevents metallic diffusion across the interface into the GaAs substrate and therefore results in an improved thermal stability (Wada *et al*., 1976).

In nanoindentation tests, a discontinuity (pop-in) event commonly occurs in the loading curve (Leipner *et al.*, 2001; Chrobak, 2007), while another discontinuity (pop-out) event is commonly seen in the unloading curve (Rao *et al.*, 2007). These discontinuities have been widely attributed to dislocation deformation and plastic deformation under the indenter (Patriarche *et al.*, 2004). The literature contains many investigations into the mechanical properties of GaAs during

nanoindentation (Leipner *et al.*, 2001). In addition, recent studies have shown that the temperature plays an important role in determining the mechanical properties of Ti/GaAs thin film systems (Leipner *et al.*, 2001; Patriarche *et al.*, 2004; Durst *et al.*, 2005). However, the effects of the annealing temperature on the plastic deformation of nanoindented Ti/GaAs thin films are still not fully clear. Accordingly, the present study investigates the mechanical properties of as-deposited Ti/GaAs thin films and Ti/GaAs thin films annealed at a temperature of 490ºC for 36 minutes by means of nanoindentation tests performed to a depth of 200 nm under room temperature (RT) conditions. The microstructures of the as-deposited and annealed Ti/GaAs films are examined using scanning electron microscopy (SEM), transmission electron microscopy (TEM) and Raman scattering spectroscopy.

THEORETICAL BACKGROUND OF NANOINDENTATION TESTS

In nanoindentation tests, the elastic modulus is generally calculated using the Oliver and Pharr equation (Pharr *et al*, 1992), i.e.,

$$\frac{1}{E_r}=\frac{(1-\nu_s^2)}{E_s}+\frac{(1-\nu_i^2)}{E_i} \quad (1)$$

where E_s and E_i are the elastic modulus values of the specimen and indenter, respectively; V_s and V_i are the Poisson ratios of the specimen and indenter, respectively; and E_r is the reduced modulus. Note that E_r accounts for the elastic deformation of the indenter, and is defined as

$$E_r=\frac{\sqrt{\pi}}{2}\frac{S}{\sqrt{A}} \quad (2)$$

where S is the contact stiffness (i.e., the slope of the load-displacement curve at the beginning of the unloading phase) and A is the projected contact area.

The indentation hardness of the sample can be obtained by dividing the maximum normal indentation load (Pmax) by the projected contact area (A), i.e.

$$H=\frac{P_{\max}}{A} \quad (3)$$

where A is determined from the area function A (h_c), which expresses the cross-sectional area of the indenter in terms of the contact depth. The actual depth of contact (h_c) is determined as

$$h_c=h_{\max}-m\varepsilon\frac{P_{\max}}{S} \quad (4)$$

where h_{max} is the maximum penetration depth of the indenter, ε is a geometrical constant associated with the indenter shape (e.g., ε=0.75 for a Berkovich indenter), and S is the contact stiffness.

Having computed h_c, the projected contact area (A) can be determined from the following fitting equation (Oliver and Pharr, 1992):

$$A=f(h_c)=24.5h_c^2+c_1h_c^1+c_2h_c^{1/2}+c_3h_c^{1/4}+\ldots+c_8h_c^{1/128} \quad (5)$$

where c_1 through c_8 are constants. Note that the first term on the right-hand side of the equation describes a perfect Berkovich indenter, while the remaining terms describe the deviation of the indenter geometry from the ideal Berkovich geometry due to tip blunting.

Ti/GaAs thin films are a binary system. Thus, the Young's modulus of the thin film is determined by both the Young's modulus of the Ti film and the Young's modulus of the GaAs substrate. The combined Young's modulus E_{eff} of the film/substrate system can be estimated as follows (Huajian *et al*, 1992):

$$E_{eff}=E_s+(E_f-E_s)I_0 \quad (6)$$

where E_s is the bulk GaAs modulus, E_f is the Ti bulk modulus, and I_0 is a function of *t/a* (with *t* being the film thickness and *a* being the contact radius). In general, when plotting the Young's modulus against the displacement for a thin film/hard substrate system such as that considered in the present study, three distinct Young's modulus regimes are observed, where each regime corresponds to a specific normalised depth (i.e. the contact depth (h_c) divided by the film thickness (t)). In the shallow penetration regime (i.e., regime I), the response is related only to the Young's modulus of the film. However, as the depth increases (i.e., regime II), the Young's modulus increases as a result of the combined effects of the thin film and substrate, respectively. Finally, at the maximum indentation depth (i.e., regime III), the Young's modulus of the thin-film system is dominated by that of the substrate.

According to Wittling *et al.* (1995) the hardness of the Ti/GaAs thin film system can be estimated as

$$H_{eff}=H_s+(H_f-H_s)\phi_H \quad (7)$$

where H_s and H_f are the hardness values of the substrate and film, respectively, and $\emptyset_H$ is one of a variety of weighting functions.

EXPERIMENTAL PROCEDURE

The Ti/GaAs specimens were prepared by depositing a Ti film with a thickness of approximately 100 nm on a GaAs substrate using an E-beam evaporation technique. During the deposition process, the substrate was rotated continuously at a speed of 30 rpm and heated at a temperature of 150ºC in order to enhance the evaporation process and

improve the uniformity of the deposited film. Following the deposition process, some of the specimens were annealed at 490ºC for 36 minutes in a thermal annealing system in order to prompt the formation of interfacial compounds (Wada *et al*., 1976; Kim, 1988; Kniffin and Helms, 1987).

The nanoindentation tests were performed using an MTS nanoindenter XP system with a Berkovich diamond pyramid tip with the indenter contact radius of 50 nm. The specimens were indented smoothly to a maximum depth of 200 nm. The indenter was held in place for 10 s and was then smoothly withdrawn. For each specimen (as-deposited and annealed), the load-displacement data were used to determine the hardness and Young's modulus of the Ti/GaAs thin film in accordance with the method described in Section 2. In order to more readily identify the indentation positions following the tests, a permanent position array system was patterned on the specimen surface using a lithography etching process (see Fig. 1(a)).

TEM foils were prepared using an FEI Helios G3CX focus ion beam (FIB) milling system with a Ga^+ ion beam and an operating voltage of 30 keV. Before the foils were milled, a thin film of Pt was deposited on the specimen surface to protect the indentation region from accidental damage by the ion beam. As shown in Fig. 1(b), the specimens were extracted in such a way as to contain the centre of the indented zone. The cross-sectional microstructures of the various specimens were observed using an EOL JEM-3010 Analytica Scanning Transmission Electron Microscope with an operating voltage of 300 kV. The formation of the compound of the samples were confirmed via Raman scattering spectroscopy performed at room temperature using a 513 nm argon laser beam.

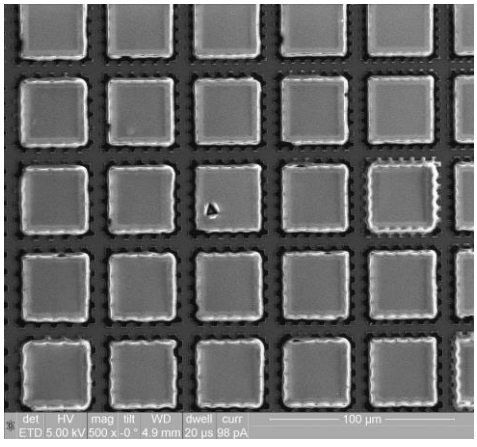

Fig. 1 (a) Original indentation positions identified using scanning electron microscopy and permanent position array system.

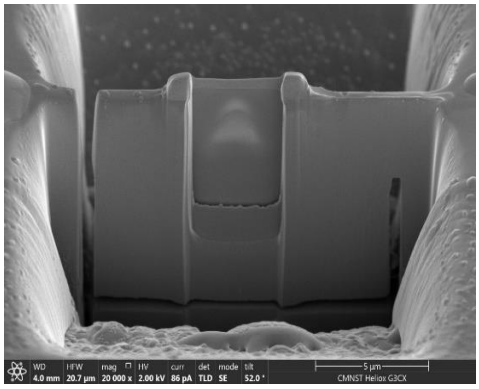

Fig. 1 (b) TEM thin foil specimen prepared using focused ion beam (FIB) milling system.

RESULTS and DISCUSSION

Loading-unloading curves and Young's modulus and hardness properties

Figures 2(a) and 2(b) show the load-displacement curves obtained for the as-deposited and annealed specimens, respectively, in the nanoindentation tests. Comparing the two figures, it is seen that the unloading curves follow the same path in both cases and are smooth and continuous, which indicates that no debonding or cracking occurs during the unloading process. However, the loading curves of the two specimens are quite different. In particular, the loading curve of the as-deposited specimen, has a discontinuity (i.e., a pop-in event) at a load of approximately 2 mN. Previous studies have attributed the pop-in event in GaAs systems to the formation of dislocations and the sudden onset of plastic deformation once the load reaches a certain critical value (Wada *et al*., 1976; Rao *et al*., 2007). By contrast, the loading curve of the annealed specimen is continuous and smooth profile with no pop-in event (Fig. 2(b)). In other words, the rate of dislocation nucleation is low and the dislocation activity is not evident as the nanoindentation load is increased.

Figures 3(a) and 3(b) show the variation of the Young's modulus with the indentation depth for the as-deposited and annealed Ti/GaAs specimens, respectively. It is found that for both samples, the Young's modulus is unstable during the initial stages of indentation due to the indentation size effect (Manika and Maniks, 2006). However, when the indenter tip is embedded entirely within the GaAs substrate, the Young's modulus stabilizes to an approximately constant value. As shown in Fig. 3(a), for indentation depths of greater than 50nm, the Young's modulus of the as-deposited Ti/GaAs specimens is around 124.01 GPa. Moreover, as shown in Fig. 3(b), for indentation depths of greater than 50nm, the Young's modulus of the annealed Ti/GaAs specimens is found to be 124.3 GPa. Comparing the Young's modulus of the as-deposited specimens with that of the annealed specimens, it is

found that the variation of the Young's modulus is annealing independent. Furthermore, the value of the Young's modulus of the as-deposited and the annealed specimens is close to that of GaAs (123±1GPa) reported by Grillo *et al.*(2003), and is similar to the value of the basal plane titanium(123 ± 5GPa) reported by Mantel *et al.* (1999).

Figures 4(a) and 4(b) show the variation of the hardness of the as-deposited and annealed specimens, respectively. As shown in Fig. 4(a), the hardness profile of the as-deposited sample has a discontinuous characteristic. Previous studies have suggested that this discontinuity arises due to the arrest of the shear band by a constant stress reduction, which is caused in turn by an increase in the average free volume inside the shear band (Yang and Nieh, 2007). The hardness of the as-deposited sample at the maximum indentation depth of 200 nm has a value of approximately 8.9 GPa, which is lower than the hardness of GaAs, i.e. 9.8 GPa (Grillo *et al.*, 2003), but higher than that of Ti film (2.1 GPa) (Mantel *et al.*, 1999) due to the presence of the Ti layer.

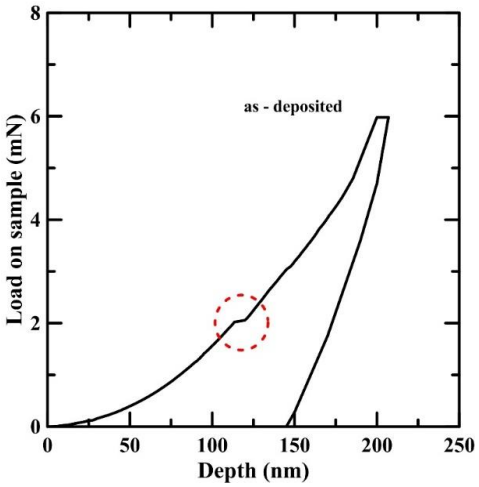

Fig. 2(a) Load-displacement curves obtained in nanoindentation tests for: (a) as-deposited specimen.

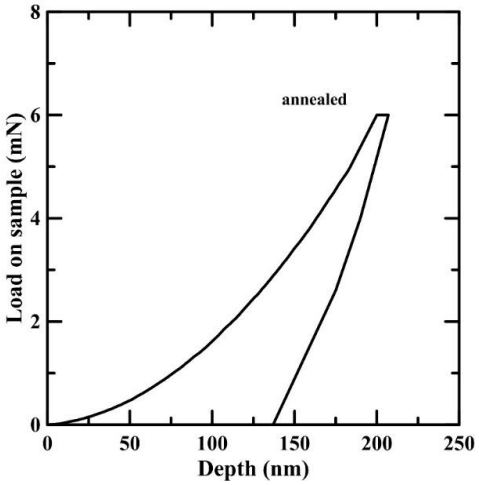

Fig. 2(b) Load-displacement curves obtained in nanoindentation tests for annealed specimen.

However, for the annealed sample (Fig. 4(b)), when indentation depths of less than 20nm, the contact force is very low and the area between the indenter and the thin film is very small. As a result, the hardness has a relatively high value of 15GPa since under low load conditions, the hardness of a material varies inversely with the contact area. However, for indentation depths of greater than 20nm, the hardness decrease rapidly to a minimum value of approximately 10.44 GPa at the maximum indentation depth of 200nm due to a metal diffusion effect between the Ti film and GaAs the substrate, i.e. the formation of the Ti_2Ga_3 and TiAs compounds formed at the interface between the Ti film and the GaAs substrate (see Section 4.2).

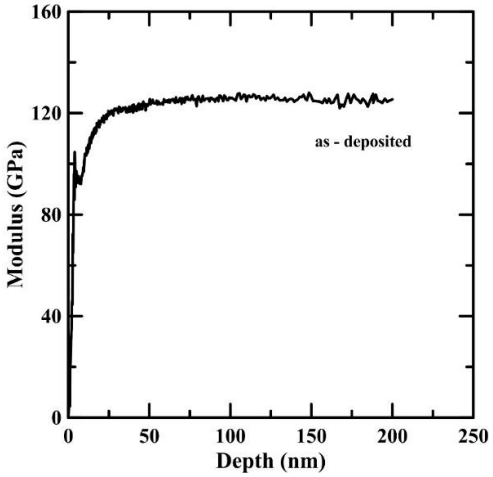

Fig. 3 (a) Modulus-displacement curves obtained in nanoindentation tests for as-deposited specimen.

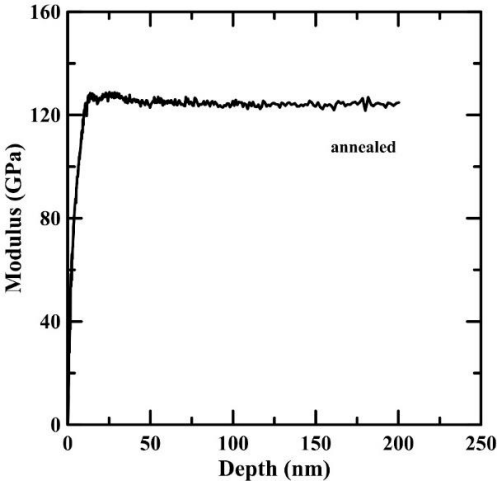

Fig. 3 (b) Modulus-displacement curves obtained in nanoindentation tests for annealed specimen.

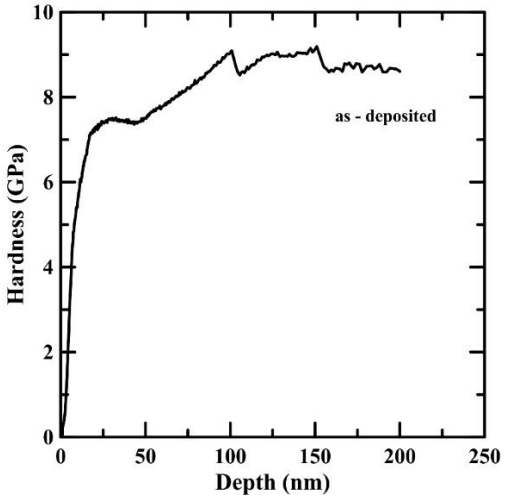

Fig. 4 (a) Hardness-displacement curves obtained in nanoindentation tests for as-deposited specimen.

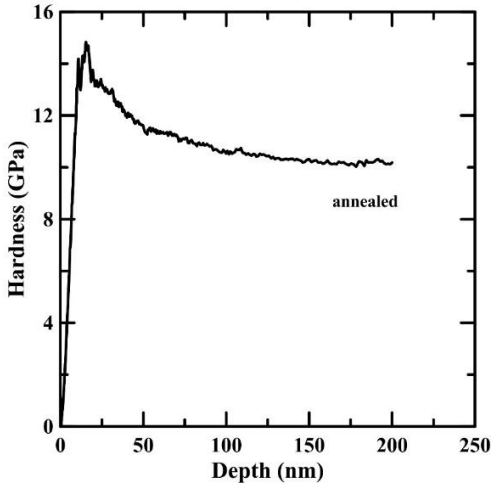

Fig. 4 (b) Hardness-displacement curves obtained in nanoindentation tests foranneal ed specimen.

TEM analysis

Figures 5(a) and 5(b) present SEM and TEM images of the indented zone in the as-deposited specimen. As expected, the indented zone has an approximately triangular shape with a maximum depth of 200 nm. It is observed that the indented microstructure contains intensive dislocation structures and the GaAs substrate undergoes plastic deformation. The dislocations provide direct evidence of the pop-in effect observed in Fig. 2(a). Figures 6(a) and 6(b) present SEM and TEM images of the indented microstructure of the annealed specimen. The indented zone again has an approximately triangular shape. However, it is shallower than that in the as-deposited specimen. The interfacial TiAs and Ti_2Ga_3 compounds are also observed as shown in Fig. 6(b). The TiAs and Ti_2Ga_3 layers have thicknesses of 35 nm and 17 nm, respectively. The formation of interfacial TiAs and Ti_2Ga_3 compounds cab be confirmed by high resolution lattice analysis by using selected area electron diffraction (SAED) patterns as shown in Fig. 9(a) latter.

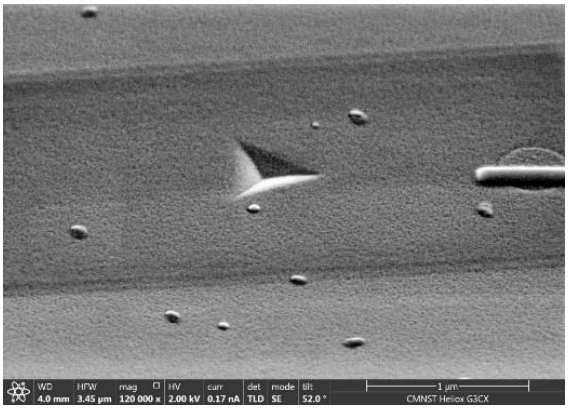

Fig. 5 (a) Micrographs of indented as-deposited specimen obtained by SEM.

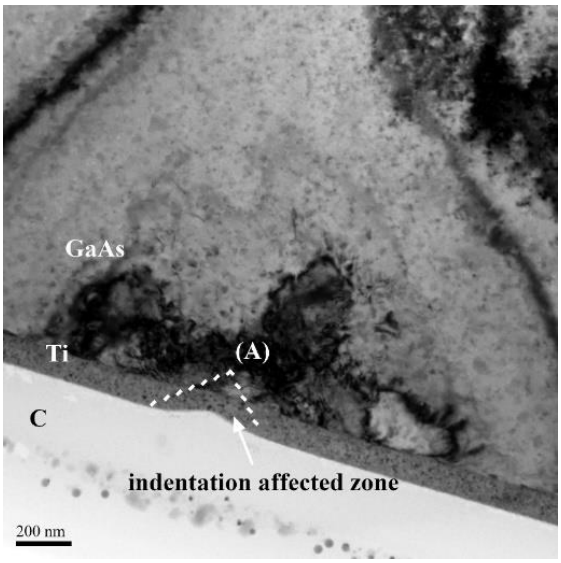

Fig. 5 (b) Micrographs of indented as-deposited specimen obtained by TEM.

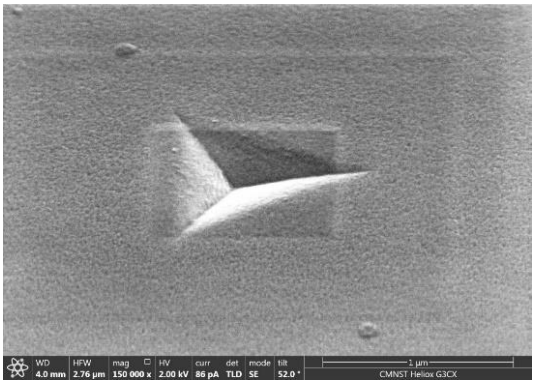

Fig. 6 (a) Micrographs of indented annealed specimen obtained by SEM.

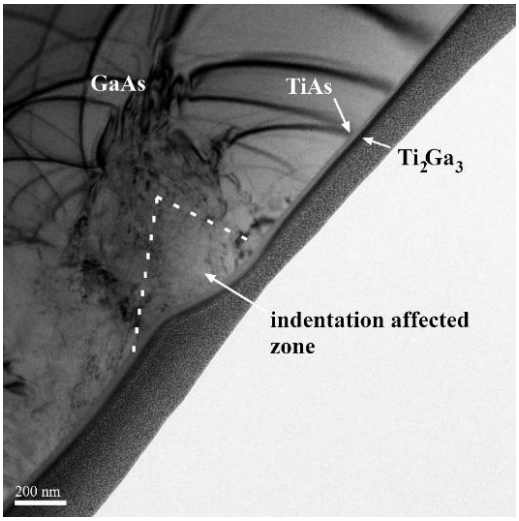

Fig. 6 (b) Micrographs of indented annealed specimen obtained byTEM.

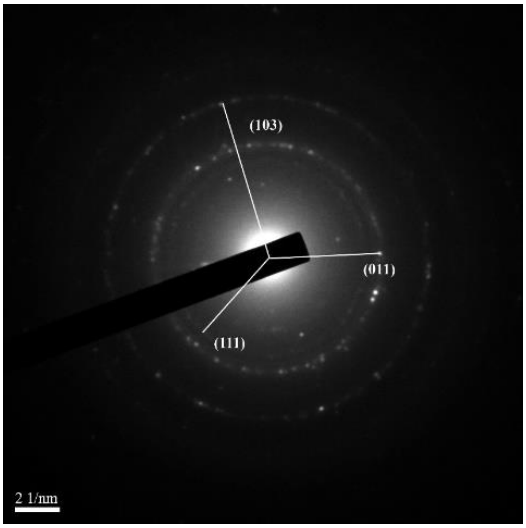

Fig. 7(a) Selected area electron diffraction (SAED) patterns of Ti film.

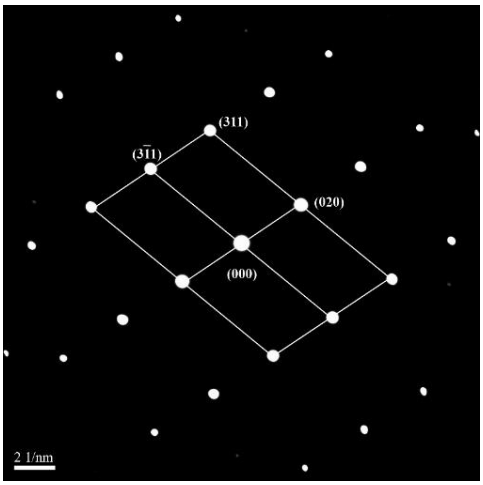

Fig. 7 (b) Selected area electron diffraction (SAED) patterns of GaAs substrate.

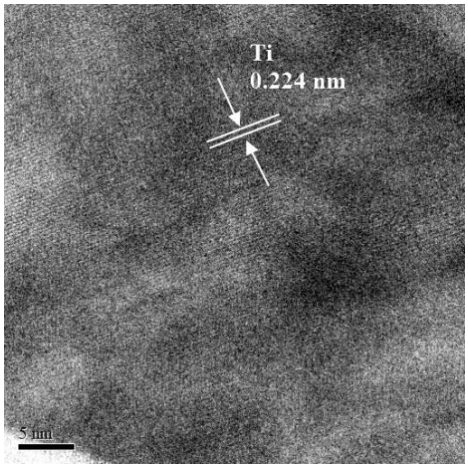

Fig. 8 (a) High-resolution TEM (HRTEM) micrographs of: Ti film.

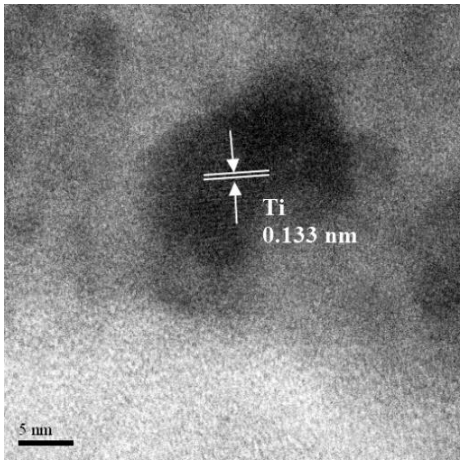

Fig. 8 (b) High-resolution TEM (HRTEM) micrographs of Ti film.

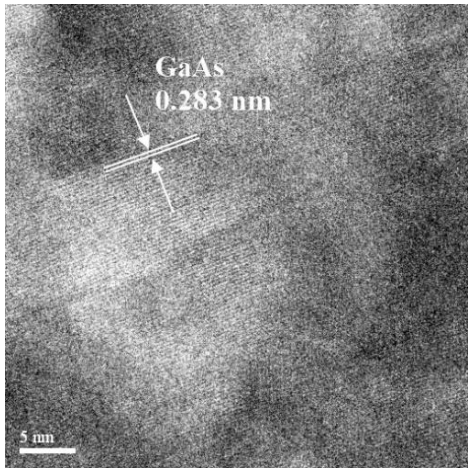

Fig. 8 (c) High-resolution TEM (HRTEM) micrographs of GaAs substrate.

Figures 7(a) and 7(b) show the selected area electron diffraction (SAED) patterns for the Ti film

and GaAs substrate, respectively. Figures 8(a), 8(b) present high-resolution TEM (HRTEM) images of the Ti film, respectively, and 8(c) for GaAs substrate. It is found that the d spacings of the Ti film are 0.224 nm, 0.133 nm, respectively, which are close to the values reported by Kim *et al.* (1988). Furthermore, for the GaAs substrate the d spacing is measured as 0.283 nm, which are close to the values reported by Kim *et al*. (1988).

Following the annealing process, the as-deposited Ti/GaAs specimen transforms to a Ti_2Ga_3/TiAs/GaAs system (see Fig. 6). Figures 9(a) and 9(b) show the d-spacings of the Ti_2Ga_3 and TiAs compounds, respectively. The d-spacing for the Ti_2Ga_3 compound is equal to 0.44 nm, while the d-spacing for the TiAs spacing are seen to be 0.282 nm and 0.183 nm, respectively. It is noted that the present results are in good agreement with those reported by Kim *et al.* (1988). As discussed above, the loading curve of the annealed sample indicates an

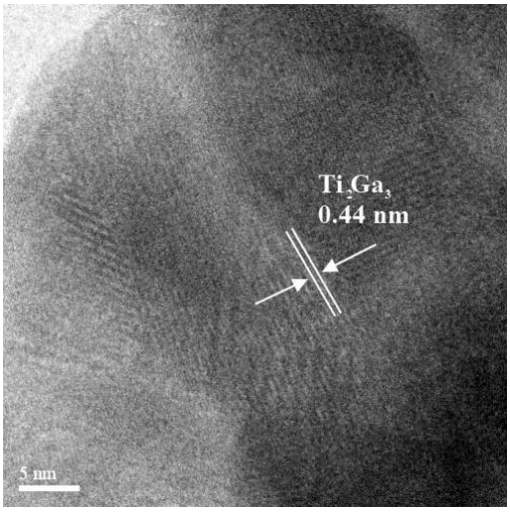

Fig. 9 (a) High-resolution TEM (HRTEM) micrographs of Ti_2Ga_3.

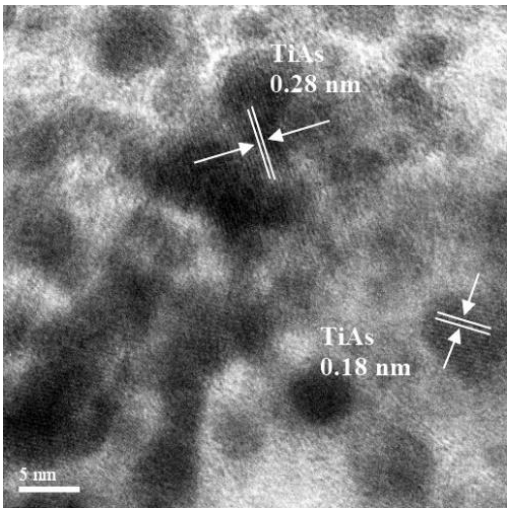

Fig. 9 (b) High-resolution TEM (HRTEM) micrographs of TiAs compound.

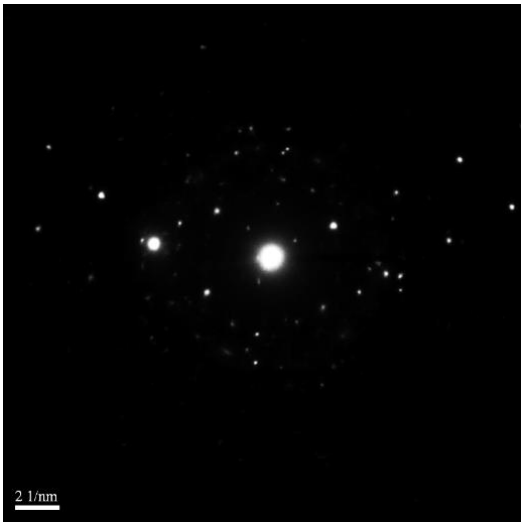

Fig. 9 (c) Selected area electron diffraction (SAED) pattern of Ti_2Ga_3/TiAs.

elastic deformation process. Thus, it is inferred that the dislocations observed in the annealed microstructure are due to a higher density of native defects or impurities in the GaAs substrate (Leipner *et al.*, 2001; Wasmer *et al.*, 2011). Figure 9(c) shows the SAED pattern of the Ti_2Ga_3 and TiAs compounds, indicating that the the Ti_2Ga_3 and TiAs compound both have a polycrystalline structure.

Raman scattering spectroscopy analysis

Figures 10(a) and 10(b) show the Raman analysis results for the GaAs substrate and the indented and annealed Ti/GaAs specimens, respectively. As shown in Fig. 10(a), the spectrum of the GaAs substrate sample contains a strong, sharp peak at 268 cm^{-1}. It is noted that a similar finding was reported by Begum *et al.* (2009) and Hilse *et al.* (2009). By contrast, the Raman spectrum of the indented and annealed specimen has a strong peak at 455 cm^{-1} (see Fig. 10(b)), which confirms the presence of the Ti_2Ga_3 compound by using high resolution lattice analysis as shown in Fig. 9(a).

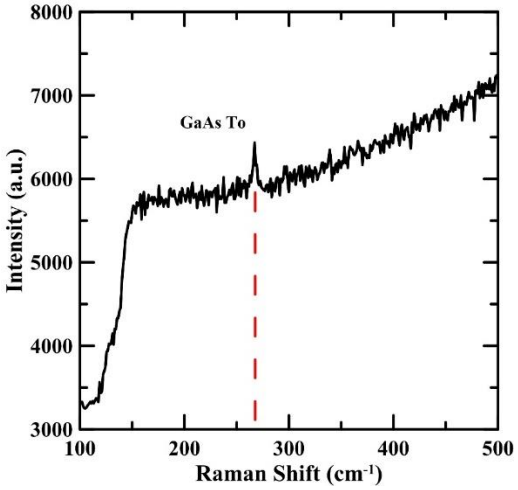

Fig. 10 (a) Fig. 10. Raman analysis of GaAs substrate.

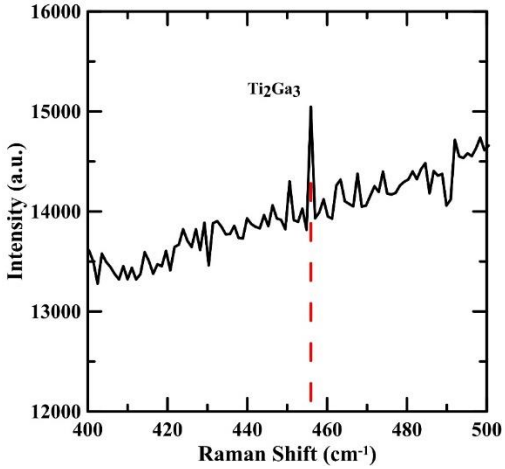

Fig. 10 (b) Fig. 10. Raman analysis of Ti_2Ga_3 layer.

CONCLUSIONS

This study has investigated the mechanical properties and microstructure of as-deposited and annealed (490ºC, 36 minutes) Ti/GaAs samples nanoindented under room temperature conditions to a maximum depth of 200 nm. The results have shown that the loading and unloading curves of the annealed specimen both have a smooth and continuous profile. In other words, the specimen undergoes elastic deformation in both the loading and the unloading stages. For the as-deposited sample, the unloading curve is also smooth and continuous. However, a pop-in event occurs during the loading process, which indicates the occurrence of plastic deformation. It has been shown that the as-deposited specimen has a maximum hardness and Young's modulus of 8.9 GPa and 124.01GPa, respectively. Moreover, the annealed specimen, have hardness values of 10.44 GPa and 124.3GPa, respectively, due to the presence of the TiAs and Ti_2Ga_3 compounds. The TEM observations have shown that both specimens contain dislocation structures in the indent-affected zone. The dislocations in the as-deposited specimen are associated with plastic deformation, while those in the annealed specimen are attributed to the presence of substrate defects. The TEM observations have also shown that the TiAs and Ti_2Ga_3 layers in the annealed specimen have thicknesses of 35 nm and 17 nm, respectively. Finally, the Raman analysis results have shown a strong peak at 268 cm^{-1} corresponding to the GaAs substrate and a strong peak at 455 cm^{-1} corresponding to the Ti_2Ga_3 compound.

ACKNOWLEDGMENT

The authors gratefully acknowledge the financial support provided to this study by the Ministry of Science and Technology (MOST) of Taiwan under Contract No. MOST 105-2221-E-006-072-MY3.

REFERENCES

Begum N., Bhatti A.S., Jabeen F., Rubini S. and Martelli F., "Lineshape analysis of Raman scattering from LO and SO phonons in III-V nanowires," Journal of Applied Physics, 106, (2009) p. 114317.

Chrobak D., K. Nordlund, and R. Nowak, "Nondislocation origin of GaAs nanoindentation pop-in event," Phys Rev Lett, 98, (2007) p. 045502.

Donzelli G. and Paccagnwlla A., "Degradation Mechanism of Ti/Au and Ti/Pd/Au Gate Metallizations in GaAs MESFET," Transactions on Electron Devices, ED-34, (1987) pp. 957-960.

Durst K., Backes B. and Göken M., "Indentation size effect in metallic materials: Correcting for the size of the plastic zone," Scripta Materialia, 52, (2005) pp. 1093-1097.

Grillo S.E., Ducarroir M., Nadal M., Tourni E. and Faurie J.P., "Nanoindentation of Si, GaP, GaAs and ZnSe single crystals," Journal of Physics D Applied Physics, 36, (2003) pp. L5-L9.

Hilse M., Takagaki Y., Herfort J., Ramsteiner M., Herrmann C., Breuer S., "Ferromagnet-semiconductor nanowire coaxial heterostructures grown by molecular-beam epitaxy," Applied Physics Letters, 95, (2009) p. 133126.

Huajian G., Cheng-Hsin C. and Jin L., "Elastic contact versus indentation modeling of multi-layered materials," International Journal of Solids and Structures, 29, (1992) pp. 2471-2492.

Kim K.B., Kniffin M., Helms C.R., "Interfacial reactions in the Ti/GaAs system," Journal of Vacuum Science & Technology A: Vacuum, Surfaces, and Films, 6, (1988) pp. 1473-1477.

Kniffin M. and Helms C.R., "Study of the structure and properties of the Ti/GaAs interface," Journal of Vacuum Science & Technology A: Vacuum, Surfaces, and Films, 5, (1987) pp. 1511-1515.

Leipner H.S., Lorenz D., Zeckzer A., Lei H. and Grau P., "Nanoindentation pop-in effect in semiconductors," Physica B: Condensed Matter, 308–310, (2001) pp. 446-449.

Manika I. and Maniks J., "Size effects in micro- and nanoscale indentation," Acta Materialia, 54, (2006) pp. 2049-2056.

Mantel F.K., Baran G.R.,and Lucas B., "Nanoindentation studies of titanium single crystals," Biomaterials, 20, (1999) pp. 1051-1055.

Nakamura T., "Mars Rover power system for solar and laser beam Utilization," Concepts and Approaches for Mars Exploration, (2012) 4043.pdf

Oliver W.C. and Pharr G.M., "An improved technique for determining hardness and elastic modulus using load and displacement sensing indentation experiments," Journal of Materials Research, 7, (1992) pp. 1564-1583.

Patriarche G., Le Bourhis E., Faurie D. and Renault P.O., "TEM study of the indentation behaviour of thin Au film on GaAs," Thin Solid Films, 460, pp. (2004) pp.150-155.

Pharr G.M., Oliver W.C. and Brotzen F.R., "On the generality of the relationship among contact stiffness, contact area, and elastic modulus during indentation," Journal of Materials Research, 7 No.3. (1992) pp.613-617.

Rao R., Bradby J.E., Ruffell S. and Williams J.S., "Nanoindentation-induced phase transformation in crystalline silicon and relaxed amorphous silicon," Microelectronics Journal, 38, (2007) pp. 722-726.

Sehgal B.K., Gulati R., Naik A.A., Vinayak Seema, Rawal D.S. and Sharma H.S., "(n)GaAs/Ti/Pt Schottky contacts and their effect on MESFET's dc parameters," Materials Science and Engineering, B48, (1997) pp. 229-233.

Sinha A.K., Smith T.E., Read M.H. and Poate J.M., "n-GaAs Schottky Diodes Metallized With Ti and Pt/Ti," Solid-State Electronics, 19, (1976) pp. 489-492.

Wada O., Yanagisawa S. and Takanashi H., "Thermal reaction of Ti evaporated on GaAs," Applied Physics Letters, 29, (1976) pp. 263-265.

Wasmer K., Gassilloud R., Michler J. and Ballif C., "Analysis of onset of dislocation nucleation during nanoindentation and nanoscratching of InP," Journal of Materials Research, 27, (2011) pp. 320-329.

Wittling M., Bendavid A., Martin P. J. and Swain M. V., "Influence of thickness and substrate on the hardness and deformation," Thin Solid Films, 270, (1995) pp. 283-288.

Yang B. and Nieh T., "Effect of the nanoindentation rate on the shear band formation in an Au-based bulk metallic glass," Acta Materialia, 55, (2007) pp. 295-300.

Yugang S., Seiyon K., Ilesanmi A. and A R.J., "Bendable GaAs metal-semiconductor field-effect transistors formed with printed GaAs wire arrays on plastic substrates," Applied Physics Letters, 87, (2005) p. 083501.

退火在鈦/砷化鎵薄膜奈米壓痕行為及化合物形成上之效應分析

李偉賢　羅崇嘉

國立成功大學機械工程系

摘要

本研究主要是探討退火在鈦/砷化鎵薄膜系統之奈米壓痕行為及薄膜界面化合物形成上的效應。本實驗首先利用電子束蒸鍍法在砷化鎵晶圓上製作一100 nm厚度之鈦薄膜，經過退火處理，條件為加熱至490℃，並持溫36分鐘，再對試片進行200 nm深度之奈米壓痕試驗，藉以瞭解退火對奈米壓痕行為及化合物形成之影響。奈米壓痕試驗結果顯示，硬度及楊氏模數受退火影響甚鉅，退火前擊退火候後之薄膜硬度值分別為8.9GPa與10.44GPa，楊氏模數則分別為124.01GPa與124.3GPa。負載-深度曲線顯示在壓痕深度200nm時，為退火的曲線有pop-in的現象發生，其原因為基材內部產生差排滑移的現象，此可由由穿透式電子顯微鏡之觀測結果得到證實。而退火試之片負載-深度曲線並無pop-in現象發生，其差排成因為基材內部雜質或空洞所致，基材並無明顯差排滑移現象產生。另由晶格間距及拉曼光譜分析可證明退火後知識片界面形成Ti2Ga3以及TiAs兩種化合物。